Ocean Modelling 178 (2022) 102098

Contents lists available at ScienceDirect

Ocean Modelling

journal homepage: www.elsevier.com/locate/ocemod

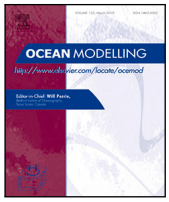

Short communication

A method for preserving nominally-resolved flow patterns in low-resolution ocean simulations: Constrained dynamics

I. Shevchenko [a,*], P. Berloff [a,b]

[a] Department of Mathematics, Imperial College London, Huxley Building, 180 Queen's Gate, London, SW7 2AZ, UK
[b] Institute of Numerical Mathematics, Russian Academy of Sciences, Gubkina 8, 119333, Moscow, Russia

ARTICLE INFO

Keywords:
Nonlinear ocean dynamics
Mesoscale eddies and their parameterizations
Dynamical systems
Constrained optimization

ABSTRACT

Inability of low-resolution ocean models to simulate many important aspects of the large-scale general circulation is a common problem. In the view of physics, the main reason for this failure are the missed dynamical effects of the unresolved small scales of motion on the explicitly resolved large-scale circulation. Complimentary to this mainstream physics-based perspective, we propose to address this failure from the dynamical systems point of view, namely, as the persistent tendency of phase space trajectories representing the low-resolution solution to escape the right region of the corresponding phase space, which is occupied by the reference eddy-resolving solution. Based on this concept, we propose to use methods of constrained optimization to confine the low-resolution solution to remain within the correct phase space region, without attempting to amend the eddy physics by introducing a process-based parameterization. This approach is advocated as a novel framework for data-driven hyper-parameterizations of mesoscale oceanic eddies in non-eddy-resolving models. We tested the idea in the context of classical, baroclinic beta-plane turbulence model and showed that non-eddy-resolving solution can be substantially improved towards the reference eddy-resolving benchmark.

1. Introduction

The problem of reproducing large-scale flow structures in low-resolution ocean simulations is among the most challenging ones in ocean modelling, and this is mostly due to the lack of information from the small, unresolved scales. The mainstream approach to this problem is to use parameterizations, that is, mathematically simple and physically justified approximations of the key unresolved and under-resolved small-scale processes (e.g., Gent and Mcwilliams (1990), Duan and Nadiga (2007), Frederiksen et al. (2012), Jansen and Held (2014), Mana and Zanna (2014), Cooper and Zanna (2015), Grooms et al. (2015), Berloff (2016, 2018), Danilov et al. (2019), Ryzhov et al. (2019), Juricke et al. (2020a,b), Cotter et al. (2019), Ryzhov et al. (2020), Cotter et al. (2020a,b,c)). Despite the decades of research effort invested in this direction, the problem remains mainly unresolved for various reasons, the majority of which is due to inaccurate description of small-scales physics and energy transfers between scales.

This work takes a new angle on this long-standing problem. Namely, we propose to look at the problem from the dynamical system point of view and consider the inability of the low-resolution model to reproduce the large-scale flow structures as the persistent tendency of phase space trajectories representing the low-resolution solution to escape the right region of the corresponding phase space, which is occupied by the reference eddy-resolving solution. Thus, instead of parameterizing directly the action of unresolved scales onto the resolved ones, our approach is to constrain the low-resolution flow dynamics to the right region of the phase space. Two other methods based on this approach were developed and tested earlier. The first method computes the low-resolution solution as the phase space trajectory of the image point, which is dynamically governed by the reference solution (Shevchenko and Berloff, 2021a). The second method reconstructs a dynamical system from the reference solution, and then explicitly uses this system to predict the low-resolutions circulation (Shevchenko and Berloff, 2022). In this study we propose a new method: the employed low-resolution model, which is integrated explicitly, is constrained by an optimization procedure that restricts the solution to stay within the right region of phase space, as defined from the reference solution. For the proof-of-concept stage, we consider, first, the Lorenz model, and, then, the classical, baroclinic quasigeostrophic (QG) model of the beta-plane turbulence.

2. The method

We run the mathematical model of the studied phenomenon (here, the QG model) at low resolution and restrict its solution to the reference

* Corresponding author.
E-mail address: i.shevchenko@imperial.ac.uk (I. Shevchenko).

https://doi.org/10.1016/j.ocemod.2022.102098
Received 17 November 2021; Received in revised form 18 May 2022; Accepted 16 August 2022
Available online 22 August 2022

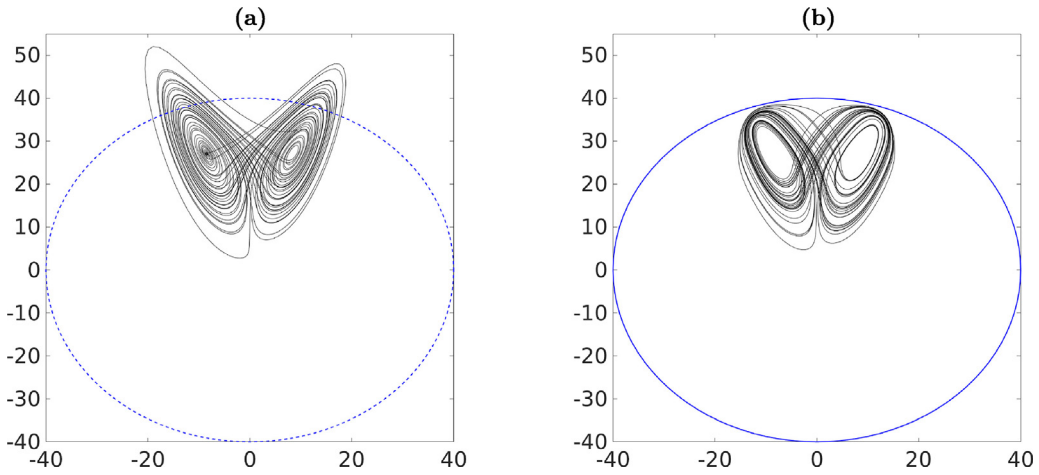

Fig. 1. Shown are **(a)** solution of the Lorenz system (3) projected on the (x, z)-plane and **(b)** the corresponding solution constrained to a ball of radius $r = 40$ (blue line) centred at $(0, 0, 0)$ for $t = [0, 50]$.

region of phase space defined by a set of constraints g (a ball of radius r in our case). The method is based on solving a constrained minimization problem of the form (e.g., Bertsekas (1996)):

$$\begin{aligned} &\min \qquad f(\mathbf{x}), \\ &\text{subject to} \quad g(\mathbf{x}) \le 0\,, \end{aligned} \tag{1}$$

where f and g are given functions. In order to inject the constraint into the minimization problem, we use the barrier function $\phi = -1/g(\mathbf{x})$, which leads to the following unconstrained minimization problem:

$$\min \quad f(\mathbf{x}) + \frac{\mu}{g(\mathbf{x})}\,, \quad \mu \to 0\,, \tag{2}$$

where parameter $\mu > 0$ regulates accuracy for finding the minimum. In our case, a very accurate approximation of the minimum is not required as the problem is chaotic, and the goal of constraining will be achieved anyway. However, we expect that a systematically wrong choice of μ over relatively long periods of time can potentially lead to a flow dynamics with different (compared to the reference solution) large-scale features not to mention small-scale ones. Without compromising the main message, we leave further technicalities beyond the scope of our work and refer readers to Bertsekas (1996).

As an example, we first consider the Lorenz 63 system (Lorenz, 1963):

$$\begin{aligned} &\mathbf{x}'(t) = \mathbf{F}(\mathbf{x}(t)), \quad \mathbf{F} := \begin{pmatrix} \sigma(y - x) \\ x(\rho - z) - y \\ xy - \beta z \end{pmatrix}, \\ &\text{subject to} \quad g(\mathbf{x}) := x^2 + y^2 + z^2 - r^2 \le 0\,, \end{aligned} \tag{3}$$

where prime denotes a derivative with respect to time, and $\mathbf{x}(t) = (x(t), y(t), z(t))$.

In order to reformulate the constrained Lorenz system (3) as an unconstrained minimization problem, we first choose an integrator (the Euler method in our case) and then define the objective function $f(\mathbf{x})$ and the constraint $g(\mathbf{x})$ as follows:

$$f(\mathbf{x}) := \frac{1}{2}\|\mathbf{x}_{n+1} - \mathbf{x}_n - \Delta t \mathbf{F}(\mathbf{x}_n)\|_2^2\,, \quad g(\mathbf{x}_{n+1}) := x_{n+1}^2 + y_{n+1}^2 + z_{n+1}^2 - r^2 \le 0\,, \tag{4}$$

where Δt is the time step, and $\mathbf{x}_n$ denotes the solution at discrete time $t_n = n\Delta t$, $n \ge 0$. The solution to the unconstrained minimization problem (2) with given functions $f(\mathbf{x})$ and $g(\mathbf{x})$ can be found with an optimization method; we use Newton's method. The initial point, $\mathbf{x}_{n+1}^0$ for the optimization method must be feasible, i.e. satisfy the constraint $g(\mathbf{x}_{n+1}^0) \le 0$; otherwise, the method fails to find the optimal solution.

In order to solve the constrained Lorenz system, we take $\sigma = 10$, $\beta = 8/3$, $\rho = 28$; and the initial condition $\mathbf{x}(t_0) = (-4.32, -6.00, 18.34)$ is chosen close to the Lorenz attractor. The results are presented in Fig. 1.

As seen in Fig. 1a, the solution to the Lorenz system remains on the attractor over the whole simulation time, and there are no constraints influencing the trajectory. If trajectory is to be restricted to some region of the phase space, then a set of constraints needs to be introduced. We chose a ball of radius $r = 40$ centred at $(0, 0, 0)$ to be the constraining phase space region, and the constrained solution remains in it over the whole simulation (Fig. 1b). But, the constrained solution is not the same as the original one even within the ball interior — the region where the trajectory is allowed to evolve with no constraints, as long as the constraints are satisfied. It happens because the constraints deform the structure of the original phase space by imposing extra restrictions on the solution. If we keep decreasing the radius, the deformation eventually becomes so large that the constrained system completely fails to reproduce the Lorenz attractor (not shown). This indicates that the Lorenz system should be somehow modified, but discussing this is beyond the scope of our study.

The above example shows how one can use the constrained optimization approach in more sophisticated settings. For instance, one can take the primitive-equations or a QG ocean model, compute its eddy-resolving reference solution, project it onto the coarse grid, and find (approximately) a spherical region of the phase space that is occupied by this solution. If the unconstrained low-resolution model configuration cannot reproduce the (nominally resolved) reference circulation, then implementation of constraint is justified, and the questions are whether it works and how can it be tuned and optimized.

3. Multilayer quasi-geostrophic equations

In this section we apply the method to the two-layer QG model describing evolution of the potential vorticity (PV) anomaly $\mathbf{q} = (q_1, q_2)$ in a domain Ω (Pedlosky, 1987):

$$\begin{aligned} &\frac{\partial q_1}{\partial t} + \mathbf{u}_1 \cdot \nabla q_1 = \nu \nabla^4 \psi_1 - \beta \frac{\partial \psi_1}{\partial x}, \\ &\frac{\partial q_2}{\partial t} + \mathbf{u}_2 \cdot \nabla q_2 = \nu \nabla^4 \psi_2 - \mu \nabla^2 \psi_2 - \beta \frac{\partial \psi_2}{\partial x}\,, \end{aligned} \tag{5}$$

where $\boldsymbol{\psi} = (\psi_1, \psi_2)$ is the velocity streamfunction in the top and bottom layers, respectively; $\beta = 2 \times 10^{-11}\,\mathrm{m^{-1}\,s^{-1}}$ is the planetary vorticity gradient; $\mu = 4 \times 10^{-9}\,\mathrm{s^{-1}}$ is the bottom friction parameter; ν is the lateral eddy viscosity (to be specified later), and $\mathbf{u} = (u, v)$ is the flow velocity vector. The ocean basin $\Omega = [0, L_x] \times [0, L_y] \times [0, H]$ is zonally periodic flat-bottom channel with horizontal dimensions $L_x = 1800$ km and $L_y = L_x/2$, with the depth $H = H_1 + H_2$, and filled out by two stacked isopycnal fluid layers of depths $H_1 = 1.0$ km and $H_2 = 3.0$ km. More details about the problem formulation, the flow dynamics in the channel and large-small scale interactions can be found in Berloff and Kamenkovich (2013b).

Forcing in (5) is introduced via a vertically sheared, baroclinically unstable, background flow (e.g., Berloff and Kamenkovich (2013a)):

$$\psi_i \to -U_i\, y + \psi_i, \quad i = 1, 2\,, \tag{6}$$

with the zonal velocities $U = [6.0, 0.0]\,\mathrm{cm\,s^{-1}}$.

The layer-wise PV anomalies and streamfunctions are related through the pair of coupled elliptic equations:

$$q_1 = \nabla^2\psi_1 + s_1(\psi_2 - \psi_1), \tag{7a}$$

$$q_2 = \nabla^2\psi_2 + s_2(\psi_1 - \psi_2)\,, \tag{7b}$$

with stratification parameters $s_1 = 4.22 \cdot 10^{-3}\,\mathrm{km^{-2}}$ and $s_2 = 1.41 \cdot 10^{-3}\,\mathrm{km^{-2}}$ chosen so that the first baroclinic Rossby deformation radius is $Rd_1 = 25\,\mathrm{km}$. The mass and momentum constraints are imposed following McWilliams (1977). System (5)–(7) is augmented by the periodic horizontal boundary conditions set at the eastern (Γ_2) and western (Γ_4) boundaries:

$$\boldsymbol{\psi}\Big|_{\Gamma_2} = \boldsymbol{\psi}\Big|_{\Gamma_4}, \quad \boldsymbol{\psi} = (\psi_1, \psi_2)\,, \tag{8}$$

and no-slip boundary conditions,

$$\boldsymbol{u}\Big|_{\Gamma_1} = \boldsymbol{u}\Big|_{\Gamma_3} = 0\,, \tag{9}$$

are imposed at the northern (Γ_1) and southern (Γ_3) boundaries. We use 513×257 uniform spatial grid, take the eddy viscosity value $\nu = 25\,\mathrm{m^2\,s^{-1}}$, and spin up the model from the state of rest to $t = 0$ over the time interval $T_{spin} = [-10, 0]\,\mathrm{years}$, so that the statistically equilibrated flow regime is established. For the low-resolution model, we use the same set-up, except for much coarser grid 129×65 and much larger eddy viscosity value $\nu = 250\,\mathrm{m^2\,s^{-1}}$. Note that dimensional units can be converted to their non-dimensional analogues by using the velocity scale $0.01\,\mathrm{m\,s^{-1}}$ and the grid interval as the length scale.

In order to apply the method to the QG equations (5) one has to choose the variable or variables to constrain. For this role we take the PV anomaly $\mathbf{q}$ that leads to the inequality $g(\mathbf{q}) \le 0$; however, the method is not limited to this particular choice, and other constraints can be implemented. For example, one can constrain the velocity field or individual terms in the equations. To solve the constrained optimization problem (2) for the QG model (5) we use the same algorithm as for the Lorenz system (3). The only difference is the time integrator, which is the Leapfrog scheme for the QG equations.

As seen in Fig. 2a, in each direction the reference solution has 4 well-pronounced horizontal jets, which the (unconstrained) low-resolution model fails to reproduce (Fig. 2b). This is because the low-resolution solution trajectory quickly escapes the right phase space region, even when we start it from the right initial condition. The phase space is constrained as

$$g(\widetilde{\mathbf{q}}) := \|\widetilde{\mathbf{q}} - \langle\mathbf{q}\rangle\|_2^2 - r^2 \le 0, \quad \langle\mathbf{q}\rangle := \frac{1}{T}\int_0^T \mathbf{q}(t)\,dt,$$
$$r := \frac{1}{T}\int_0^T \|\mathbf{q}(t) - \langle\mathbf{q}\rangle\|_2\,dt\,, \tag{10}$$

where $r = 846$ (non-dimensional units), $T = 4$ years, and $\widetilde{\mathbf{q}}$ denotes the constrained low-resolution solution restricted to the ball of radius r. Constraint (10) corresponds to the ball of radius r centred at the 4-year time mean of the reference eddy-resolving solution $\langle\mathbf{q}\rangle$; and the radius is found as the mean distance of the 4-year long reference solution from $\langle\mathbf{q}\rangle$. Here, the ball is the simplest approximation of the real reference-solution attractor in the phase space. It might seem reasonable to find a value of r such that the low-resolution constrained solution $\widetilde{\mathbf{q}}$ is a more accurate approximation to the reference solution $\mathbf{q}$. However, we do not recommend this, since r is an approximation to the reference phase volume, i.e. even knowing its optimal value does not guarantee a significantly more accurate solution, as the coarse-grain trajectory may not visit the attractor regions populated by the reference solution. A better way would be to more accurately approximate the shape of the reference phase space volume. For example, one could find a hyper-ellipsoid that takes into account the actual spread of the attractor along different coordinate axes.

When the model is constrained, the 4 jets in the top layer are recovered both in the instantaneous and time-mean fields (Fig. 2c). The relative blurriness of the jet edges comes from the use of an order-of-magnitude larger viscosity. Perhaps, the jet edges can be sharpened up by injecting noise into the advection operator, as in the SALT approach (e.g. Cotter et al. (2019, 2020a,b,c)), or simply by adding it as a forcing. On the other hand, the jets in the bottom layer are much weaker compared to those in the top layer but even in this case the constrained model reproduces them, although these jets are less smeared compared to the reference ones. We hypothesize that our approximation of the reference phase space is too rough to accurately capture the jets in the bottom layer.

To see how the radius of the ball influences the dynamics, we took the ball of a larger radius $r = 923$ (this is the maximum radius for the 10-year-long reference solution). In this case, the constrained solution still has the jets, which are, however, noticeably corrupted (Fig. 2d), especially after 10 years of simulation (see the jet near the southern boundary). However, the 10-year average of the bottom layer PV anomaly (Fig. 2d) shows relatively good agreement with the reference solution (Fig. 2a), with particular improvement over the $r = 846$ case (Fig. 2c). This indicates that increasing the radius improves the representation of the PV anomaly mean field in the bottom layer (the 10 year average). This contrasts with the observed behaviour of the upper layer when increasing the radius, which corrupts the PV anomaly fields in the upper layer. It suggests that the ball of a fixed radius is likely not the most appropriate representation of the shape of reference phase space. On the other note, the separation between the two southern jets becomes less evident (see the time-average subplot) and the standard deviation does not show as pronounced jets as those of the reference solution or the solution constrained in the smaller ball. This is explained by the fact that the solution constrained by a larger ball drifts farther away from the right phase space region. Based on this evidence, one could think that a tighter ball would yield a more accurate solution, but this is not necessarily the case, since an over-constrained QG model can lead to significantly incorrect dynamics. As an example, we found the solution for $r = 796$ (this is the minimum radius for the 10-year-long reference solution) and obtained the results very similar to those with $r = 846$ (not shown). This another suggestion that the ball is not an accurate approximation of the reference phase space when finer structures of the solution have to be modelled. As an alternative, one should focus on methods that can better approximate the reference phase space.

In order to get better insights in the low-resolution dynamics in the phase space we compute the Euclidean distance $D(t)$ of different solutions from the reference time mean (Fig. 3).

As it follows from the results the constrained low-resolution solution evolves near the boundary of the constrained region, since the low-resolution solution (Fig. 2b) is too crude an approximation to the reference solution (Fig. 2a), and therefore the low-resolution solution always tries to escape the constrained region. However, even in this case the method restores the nominally-resolved flow patterns that are not present in the unconstrained low-resolution solution.

4. Conclusions and discussion

In this work we have further developed alternative hyper-parameterization approach for parameterizing effects of mesoscale oceanic eddies on the large-scale ocean circulation. Complimentary to the mainstream physics-based perspective, we propose to deal with the eddy effects from the dynamical systems point of view, and interpret the lack of them as the persistent tendency of phase space trajectories representing the low-resolution solution to escape the right region of the corresponding phase space, which is occupied by the reference

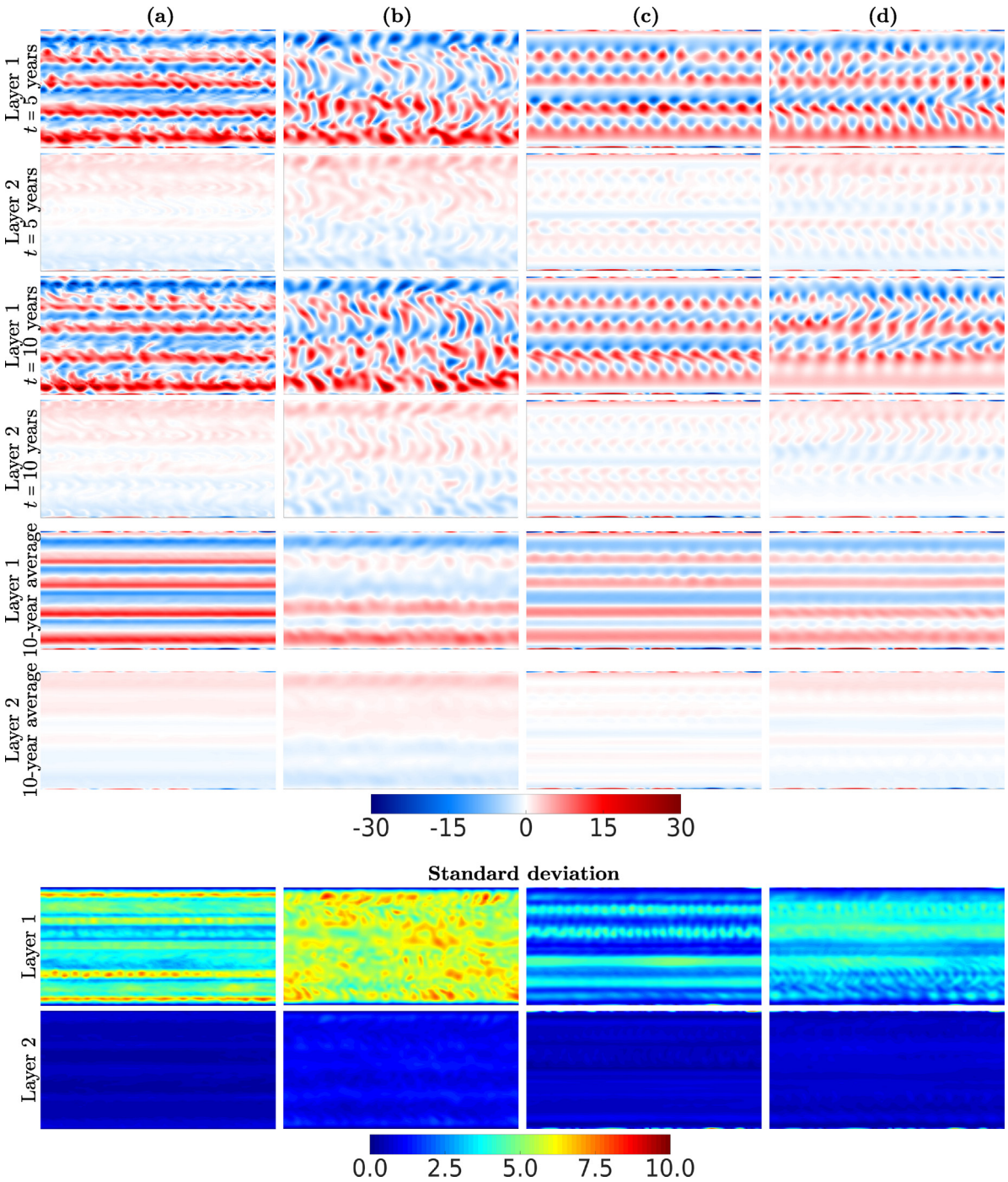

Fig. 2. Shown are snapshots of the PV anomaly and standard deviation calculated for each simulation of: **(a)** the reference solution $\mathbf{q}$ (computed with $\nu = 25\,\mathrm{m}^2\,\mathrm{s}^{-1}$ on the grid 513×257 and then projected on the grid 129×65); **(b)** the unconstrained low-resolution solution $\overline{\mathbf{q}}$ (computed on the coarse grid 129×65 with $\nu = 250\,\mathrm{m}^2\,\mathrm{s}^{-1}$); **(c)** the constrained low-resolution solution, $\widetilde{\mathbf{q}}$, restricted to the ball of radius $r = 846$ (non-dimensional units); **(d)** the same as **(c)** but for $r = 923$. The time-mean $\langle \mathbf{q} \rangle$ in (10) is kept constant for different values of r. Units of the PV anomaly fields are non-dimensional. Note that the constrained solution **(c)** preserves the nominally-resolved flow structures (the 4 jets) both in the snapshots and time mean, whereas the unconstrained one fails on this **(b)**.

eddy-resolving solution. Based on this concept, we propose to use methods of constrained optimization to confine the low-resolution solution to remain within the correct phase space region, without attempting to amend the eddy physics by introducing a process-based parameterization. Formally speaking, the constrained optimization can be thought of as being a generalization of the classical nudging approach when the solution is nudged to a reference volume in phase space with the nudging parameter tending to infinity at the boundary of the sphere; in the classical nudging the solution is nudged to a reference solution (not to a reference volume) and the nudging parameter is supposed to be fixed. It is worth mentioning that the development of such a nudging method can involve a highly-sophisticated control of the nudging parameter (or parameters) that should, probably, reflect the structure of the reference phase space.

We used the Lorenz 63 system as a simple conceptual toy model for the proof of concept. Then, we considered the baroclinic, quasi-geostrophic (QG) model of the beta-plane turbulence and showed that the low-resolution solution cannot reproduce such nominally-resolved

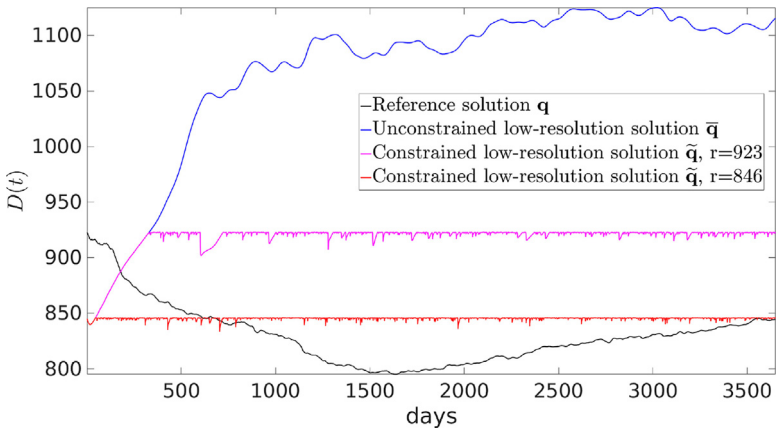

Fig. 3. Shown is the Euclidean distance $D(t)$ for the reference solution $\mathbf{q}$ (black), unconstrained low-resolution solution $\tilde{\mathbf{q}}$ (blue), constrained low-resolution solution $\tilde{\mathbf{q}}$ for $r = 923$ (magenta), and constrained low-resolution solution $\tilde{\mathbf{q}}$ for $r = 823$ (red). The unconstrained solution evolves far away from the reference time mean while the constrained solutions are much closer to the reference time mean (depending on the radius) but they evolve in the neighbourhood of the boundary of the constrained region.

flow structures, as the multiple alternating zonal jets, which are robustly present in the reference eddy-resolving solution. Implementation of the proposed hyper-parameterization approach significantly improves the low-resolution model and recovers the top-layer jets. The bottom-layer jets are much weaker compared to the top-layer ones, but even in this case the constrained model reproduces them too. However, the reference bottom-layer jets are more defused than those of the constrained model. There might be two reasons for that. Firstly, the viscosity in the constrained model is one order of magnitude larger compared to that in the reference model. It can significantly change both the dimension and structure of the attractor (compared to the reference) that leads to the second reason. Namely, our approximation of the reference phase space might be too rough (we used a ball, with the radius found as the time-mean distance of the 4-year-long reference solution from its time mean, and centred at the 4-year time mean of the reference solution) to accurately capture the jets in the bottom layer. This suggests that a more accurate approximation of the reference phase space might be needed to accurately represent the flow dynamics in the deep ocean.

It is worth drawing reader's attention to the fact that only 4 years of the reference solution have been used to find the centre of the ball and its radius, and this turned out to be enough to reproduce the jets in the 10-year-long run at low resolution. This demonstrates that the proposed method gives robust results, as soon as it is supplied with sufficient data. On the other hand, for more sophisticated models or even for different setups of the QG model, longer or shorter runs might be needed to accurately estimate the centre and radius.

In addition, we have studied how the radius of the ball influences the ability of the constrained QG model to reproduce nominally-resolved structures and found that too large radius eventually lead to the solution degradation, due to the detrimental drift in the phase space, whereas too small radius does not allow for an accurate approximation of the shape of the reference phase space. Thus, there is the optimal strength of the constraint. The analysis of the constrained solution shows that it evolves near the boundary of the constrained region, as its dynamics is governed by the low-resolution QG model which is too crude an approximation to the reference solution, and therefore the constrained solution always tries to escape the constrained region. However, even in this case the method restores the nominally-resolved flow patterns (that are not present in the unconstrained low-resolution solution) thus giving another level of reassurance that it will likely work well in more sophisticated settings.

The utility of the proposed method is that it does not require in-depth physical knowledge of interactions between the scales of motion, and it does not require any modification of the governing equations, as in the case of traditional parameterizations. The method falls into the category of data-driven methods as it requires either observations or their substitute in terms of some eddy-resolving solution data. In this work we use the projection of the high-resolution solution on the coarse grid (which we refer to as the reference solution) to compute the radius of the sphere (the boundary for the constrained optimization) and its centre in the reference phase space. If this information can be obtained without computing the reference solution (for example, through physical insights or using observational data) then the high-resolution solution is not needed. Obviously, the advantage of the method may turn into a possible drawback, as often information presented in data is not sufficient (for example, characteristics of the constraining ball may be inaccurately estimated). This can be mitigated by using more accurate approximations of the constraining geometry (for example, a hyper-ellipsoid instead of the ball to take into account the spread of the solution along different coordinate axes) and of the attractor reconstruction. Another intriguing avenue for future research extension is the so called term-wise constraining, which deals with individual dynamical terms, rather than with the whole solution, like in this study.

The proposed method can be implemented into the dynamic core of oceanic general circulation models by constraining solutions of different equations and terms, or their combinations. This is, in turn, the open broad research agenda on the effects of different data-driven constraints of the governing equations (e.g., Shevchenko and Berloff (2021c)). It can also be applied to comprehensive ocean–atmosphere models with many dynamical variables, changing external conditions, and different dynamical regimes. These models can be thought of as being either monostable chaotic systems (chaotic systems with only one chaotic attractor) or multistable chaotic systems (chaotic systems with several chaotic attractors for a given set of parameters). In case of monostable systems, different dynamical regimes are realized in different regions of one attractor. When the solution switches between different regions of the attractor it is observed as a different dynamical regime. In case of multistable systems, the solution switches between different attractors. The method should properly approximate the reference solution for monostable systems, if the coarse-grid trajectory can visit the regions of the attractor corresponding to different dynamical regimes. The method can also be used for multistable systems given that the chaotic attractors are present in the data provided. The accuracy of the method for monostable and multistable systems can be improved if combined with parameterizations of the coarse-grid model.

On the other note, the attractor might be extremely complex in a more complicated model, and it is not clear that defining a ball or ellipsoid would yield a useful constraint. Assuming more detailed knowledge of the structure of the attractor requires further knowledge of the reference flow dynamics, potentially making it more difficult to configure the method. All-in-all, the accuracy of the method for comprehensive ocean–atmosphere models remains uncharted territory worth exploring in the future.

CRediT authorship contribution statement

I. Shevchenko: Conceptualization, Methodology, Software, Validation, Formal analysis, Writing – original draft. **P. Berloff:** Writing – review & editing, Funding acquisition.

Declaration of competing interest

The authors declare that they have no known competing financial interests or personal relationships that could have appeared to influence the work reported in this paper.

Acknowledgements

The authors thank The Leverhulme Trust for the support of this work through the grant RPG-2019-024, and the anonymous referees for their constructive comments, suggestions, and efforts which helped us improve the paper. Pavel Berloff was supported by the NERC grant NE/T002220/1 and by the Moscow Centre for Fundamental and Applied Mathematics (supported by the Agreement 075-15-2019-1624 with the Ministry of Education and Science of the Russian Federation). We thank the Associate Editor David Marshall for all his work in managing this paper.

References

Berloff, P., 2016. Dynamically consistent parameterization of mesoscale eddies. Part II: eddy fluxes and diffusivity from transient impulses. Fluids 1, 1–19.
Berloff, P., 2018. Dynamically consistent parameterization of mesoscale eddies. Part III: Deterministic approach. Ocean Model. 127, 1–15.
Berloff, P., Kamenkovich, I., 2013a. On spectral analysis of mesoscale eddies. Part I: Linear analysis. J. Phys. Oceanogr. 43, 2505–2527.
Berloff, P., Kamenkovich, I., 2013b. On spectral analysis of mesoscale eddies. Part II: Nonlinear analysis. J. Phys. Oceanogr. 43, 2528–2544.
Bertsekas, D., 1996. Constrained Optimization and Lagrange Multiplier Methods, first ed. In: Optimization and Neural Computation Series, Athena Scientific.
Cooper, F., Zanna, L., 2015. Optimization of an idealised ocean model, stochastic parameterisation of sub-grid eddies. Ocean Model. 88, 38–53.
Cotter, C., Crisan, D., Holm, D., Pan, W., Shevchenko, I., 2019. Numerically modelling stochastic Lie transport in fluid dynamics. Multiscale Model. Simul. 17, 192–232.
Cotter, C., Crisan, D., Holm, D., Pan, W., Shevchenko, I., 2020a. A particle filter for stochastic advection by Lie transport (SALT): A case study for the damped and forced incompressible 2D Euler equation. SIAM/ASA J. Uncertain. Quantif. 8, 1446–1492.
Cotter, C., Crisan, D., Holm, D., Pan, W., Shevchenko, I., 2020b. Data assimilation for a quasi-geostrophic model with circulation-preserving stochastic transport noise. J. Stat. Phys. 179, 1186–1221.
Cotter, C., Crisan, D., Holm, D., Pan, W., Shevchenko, I., 2020c. Modelling uncertainty using stochastic transport noise in a 2-layer quasi-geostrophic model. Found. Data Sci. 2, 173–205.
Danilov, S., Juricke, S., Kutsenko, A., Oliver, M., 2019. Toward consistent subgrid momentum closures in ocean models. In: Eden, C., Iske, A. (Eds.), Energy Transfers in Atmosphere and Ocean. Springer-Verlag, pp. 145–192.
Duan, J., Nadiga, B., 2007. Stochastic parameterization for large eddy simulation of geophysical flows. Proc. Amer. Math. Soc. 135, 1187–1196.
Frederiksen, J., O'Kane, T., Zidikheri, M., 2012. Stochastic subgrid parameterizations for atmospheric and oceanic flows. Phys. Scr. 85, 068202.
Gent, P., Mcwilliams, J., 1990. Isopycnal mixing in ocean circulation models. J. Phys. Oceanogr. 20, 150–155.
Grooms, I., Majda, A., Smith, K., 2015. Stochastic superparametrization in a quasi-geostrophic model of the Antarctic Circumpolar Current. Ocean Model. 85, 1–15.
Jansen, M., Held, I., 2014. Parameterizing subgrid-scale eddy effects using energetically consistent backscatter. Ocean Model. 80, 36–48.
Juricke, S., Danilov, S., Koldunov, N., Oliver, M., Sein, D., Sidorenko, D., Wang, Q., 2020a. A kinematic kinetic energy backscatter parametrization: From implementation to global ocean simulations. J. Adv. Model. Earth Syst. 12, 2020MS002175.
Juricke, S., Danilov, S., Koldunov, N., Oliver, M., Sidorenko, D., 2020b. Ocean kinetic energy backscatter parametrization on unstructured grids: Impact on global eddy-permitting simulations. J. Adv. Model. Earth Syst. 12, 2019MS001855.
Lorenz, E., 1963. Deterministic nonperiodic flow. J. Atmos. Sci. 20, 130–141.
Mana, P., Zanna, L., 2014. Toward a stochastic parameterization of ocean mesoscale eddies. Ocean Model. 79, 1–20.
Pedlosky, J., 1987. Geophysical Fluid Dynamics. Springer-Verlag, New York.
Ryzhov, E., Kondrashov, D., Agarwal, N., Berloff, P., 2019. On data-driven augmentation of low-resolution ocean model dynamics. Ocean Model. 142, 101464.
Ryzhov, E., Kondrashov, D., Agarwal, N., McWilliams, J., Berloff, P., 2020. On data-driven induction of the low-frequency variability in a coarse-resolution ocean model. Ocean Model. 153, 101664.
Shevchenko, I., Berloff, P., 2021a. A method for preserving large-scale flow patterns in low-resolution ocean simulations. Ocean Model. 161, 101795.
Shevchenko, I., Berloff, P., 2021c. On a minimum set of equations for parameterisations in comprehensive ocean circulation models. Ocean Model. 168, 101913.
Shevchenko, I., Berloff, P., 2022. A method for preserving nominally-resolved flow patterns in low-resolution ocean simulations: dynamical system reconstruction. Ocean Model. 170, 101939.